ORIGINAL ARTICLE

Characterization of *MET* Exon 14 Skipping Alterations (in NSCLC) and Identification of Potential Therapeutic Targets Using Whole Transcriptome Sequencing

So Yeon Kim, MD,[a,b] Jun Yin, MD,[c] Stephen Bohlman, MD, PhD,[a] Phillip Walker, PhD,[c] Sanja Dacic, MD, PhD,[b] Chul Kim, MD,[d] Hina Khan, MD,[e] Stephen V. Liu, MD,[d] Patrick C. Ma, MD,[f] Misako Nagasaka, MD, PhD,[g] Karen L. Reckamp, MD,[h] Jim Abraham, PhD,[c] Dipesh Uprety, MD,[i] Feng Wang, PhD,[a] Joanne Xiu, PhD,[c] Jian Zhang, PhD,[c] Haiying Cheng, MD, PhD,[a] Balazs Halmos, MD[a,*]

[a]*Department of Medical Oncology, Montefiore Medical Center, Albert Einstein Cancer Center, Bronx, New York*
[b]*Yale School of Medicine, New Haven, Connecticut*
[c]*Caris Life Sciences, Phoenix, Arizona*
[d]*Georgetown Lombardi Comprehensive Cancer Center, Washington, District of Columbia*
[e]*Warren Alpert Medical School of Brown University, Providence, Rhode Island*
[f]*Penn State Cancer Institute, Hershey, Pennsylvania*
[g]*UCI School of Medicine, Orange, California*
[h]*Cedars-Sinai Medical Center, Los Angeles, California*
[i]*Karmanos Cancer Center, Detroit, Michigan*

Received 25 May 2022; revised 6 July 2022; accepted 7 July 2022
Available online - 22 July 2022

ABSTRACT

Introduction: Genomic alterations in the juxtamembrane exon 14 splice sites in NSCLC lead to increased MET stability and oncogenesis. We present the largest cohort study of *MET* Exon 14 (*MET*ex14) using whole transcriptome sequencing.

Methods: A total of 21,582 NSCLC tumor samples underwent complete genomic profiling with next-generation

*Corresponding author.

Drs. Kim and Yin contributed equally as co-first authors.

Disclosures: *Dr. Dacic has received consulting fees from AstraZeneca, has received honoraria from Takeda and Merck, and participates in the Pulmonary Pathology Society. Dr. Kim has received institutional grants from AstraZeneca, Bristol-Myers Squibb, Novartis, Regeneron, Karyopharm, Debiopharm, Janssen, Genentech, Spectrum, and Merck and has received consulting fees from AstraZeneca, Novartis, Janssen, PierianDx, Sanofi, Diffusion Pharmaceuticals, Mirati, and Jazz Pharmaceuticals. Dr. Khan has received a grant from Bristol-Myers Squibb/Winn CDA and consulting fees from Sanofi-Genzyme. Dr. Liu has received grants from Alkermes, Bayer, Blueprint, Bristol-Myers Squibb, Elevation Oncology, Genentech, Gilead, Merck, Merus, Nuvalent, Pfizer, Rain Therapeutics, RAPT, and Turning Point Therapeutics; has received consulting fees from Amgen, AstraZeneca, Bayer, Beigene, Blueprint, Boehringer Ingelheim, Bristol-Myers Squibb, Catalyst, Daiichi Sankyo, Eisai, Elevation Oncology, Genentech/Roche, Gilead, Guardant Health, Janssen, Jazz Pharmaceuticals, Lilly, Merck/Merck Sharp & Dohme, Novartis, Regeneron, Sanofi, Takeda, and Turning Point Therapeutics; and took part in data safety monitoring for Candel Therapeutics. Dr. Ma has received institutional grants from Merck, Genentech-Roche, AbbVie, Apollomics, OncoC4, Genmab, BeiGene, Mirati, and Elevation Oncology; has received consulting fees and honoraria from AstraZeneca; and is a Steering Committee Member for Big Ten Cancer Research Consortium. Dr. Nagasaka has received consulting fees from AstraZeneca, Caris Life Sciences, Daiichi Sankyo, Novartis, EMD Serono, Janssen, Pfizer, Lilly, Genentech, and Mirati; honoraria from Takeda and Blueprint; and support for attending meetings from AnHeart. Dr. Reckamp has received institutional grants from Genentech, Blueprint, Calithera, Daiichi Sankyo, Elevation Oncology, and Janssen and consulting fees from Amgen, AstraZeneca, Blueprint, Daiichi Sankyo, EMD Serono, Genentech, GlaxoSmithKline, Janssen, Lilly, Merck KGA, Mirati, Seattle Genetics, Takeda, and Tesaro. Dr. Uprety has received consultant fees from AstraZeneca, Daiichi Sankyo, and Sanofi. Dr. Halmos has received grants from Boehringer Ingelheim, AstraZeneca, Merck, Bristol-Myers Squibb, Advaxis, Amgen, AbbVie, Daiichi, Pfizer, GlaxoSmithKline, Beigene, and Janssen; has received consultant fees from Veracyte; and is part of the advisory board for AstraZeneca, Boehringer Ingelheim, Apollomics, Janssen, Takeda, Merck, Bristol-Myers Squibb, Genentech, Pfizer, Eli-Lilly, and TPT. The remaining authors declare no conflict of interest.*

Address for correspondence: Balazs Halmos, MD, Montefiore Medical Center, Albert Einstein Cancer Center, Bronx, New York. E-mail: bahalmos@montefiore.org

Cite this article as: Kim SY, Yin J, Bohlman S, et al. Characterization of *MET* exon 14 skipping alterations (in NSCLC) and identification of potential therapeutic targets using whole transcriptome sequencing. *JTO Clin Res Rep*. 2022;3:100381.

ISSN: 2666-3643

https://doi.org/10.1016/j.jtocrr.2022.100381

sequencing of DNA (592 Gene Panel, NextSeq, whole exome sequencing, NovaSeq) and RNA (NovaSeq, whole transcriptome sequencing). Clinicopathologic information including programmed death-ligand 1 and tumor mutational burden were collected and RNA expression for mutation subtypes and *MET* amplification were quantified. Immunogenic signatures and potential pathways of invasion were characterized using single-sample gene set enrichment analysis and mRNA gene signatures.

Results: A total of 533tumors (2.47%) with *MET*ex14 were identified. The most common alterations were point mutations (49.5%) at donor splice sites. Most alterations translated to increased *MET* expression, with *MET* co-amplification resulting in synergistic increase in expression ($q < 0.05$). Common coalterations were amplifications of *MDM2* (19.0% versus 1.8% wild-type [WT]), *HMGA2* (13.2% versus 0.98% WT), and *CDK4* (10.0% versus 1.5% WT) ($q < 0.05$). High programmed death-ligand 1 $\geq$ 50% (52.5% versus 27.3% WT, $q < 0.0001$) and lower proportion of high tumor mutational burden ($\geq$10 mutations per megabase, 8.3% versus 36.7% WT, $p < 0.0001$) were associated with *MET*ex14, which were also enriched in both immunogenic signatures and immunosuppressive checkpoints. Pathways associated with *MET*ex14 included angiogenesis and apical junction pathways ($q < 0.05$).

Conclusions: *MET*ex14 splicing alterations and *MET* co-amplification translated to higher and synergistic *MET* expression at the transcriptomic level. High frequencies of *MDM2* and *CDK4* co-amplifications and association with multiple immunosuppressive checkpoints and angiogenic pathways provide insight into potential actionable targets for combination strategies in *MET*ex14 NSCLC.

Keywords: METex14; Non–small cell lung cancer; Whole transcriptome sequencing; RNA expression; MDM2; Immune signatures

Introduction

The *MET* proto-oncogene plays a key role in cellular proliferation, invasion, and metastases and has been reported to play an oncogenic role in NSCLC.[1–4] Located on chromosome 7q21–31, the *MET* gene encodes a receptor tyrosine kinase, which on ligand binding with its natural ligand hepatocyte growth factor or scatter factor leads to receptor dimerization, activation of the tyrosine kinase domain, and downstream signaling of RAS/RAF/MEK and PI3K/AKT/mTOR pathways.[5] Tight regulation of *MET* expression occurs by means of the Y1003 loci located in the juxtamembrane domain encoded by exon 14. On binding of Cbl-E3 ubiquitin to Y1003, the receptor undergoes internalization and proteasomal degradation.[5] Somatic mutations at or near splicing regions of exon 14 lead to skipping of transcription of exon 14, yielding the *MET* exon 14 (*MET*ex14) alternative splicing variant with increased receptor stability and downstream oncogenic signaling.[1,6]

*MET*ex14 represents approximately 2% to 4% of metastatic NSCLC and has been associated with older age, female sex, sarcomatoid histology, and generally portends a poor prognosis.[2,3,7–9] Capmatinib and tepotinib have been Food and Drug Administration approved for MET-directed therapy in *MET*ex14-driven metastatic NSCLC on the basis of response rates of 68% and 43% in treatment-naive patients.[10–12] Although high programmed death-ligand 1 (PD-L1) has been observed with *MET*ex14, inconsistent responses to immunotherapy have been observed.[13,14] Given the aggressive nature of this key lung cancer molecular subtype and modest, variable and transient benefits with currently available agents, novel opportunities for treatment intervention through better understanding of disease biology remain a great unmet need.

Diverse genomic alterations associated with *MET*ex14 have been characterized through DNA profiling, but these assays remain an imperfect tool for identifying skipped variants as false-negative results may occur.[2–4,13,15–17] RNA sequencing has improved sensitivity in identifying skipped variants,[15,16] and to our knowledge, characterization of genomic alterations of *MET*ex14 using whole transcriptome sequencing (WTS) has yet to be reported. We have conducted preclinical assays on clustered, regularly interspaced, short palindromic repeat-modified cellular models of *MET*ex14-driven lung cancer and have found that *MET*ex14 NSCLC cells were associated with pathways related to cytoskeletal remodeling, cellular adhesion, epithelial to mesenchymal transition (EMT), and angiogenesis.[18] The in vivo up-regulation and biological role of these pathways in *MET*ex14-driven lung cancers remain to be understood and may open novel avenues for more effective and durable therapeutic interventions.

We report the largest WTS cohort defining genomic alterations and co-alterations associated with *MET*ex14 and characterize the immune microenvironment of *MET*ex14 NSCLC using a real-world database. We also report key biological processes that may be involved in invasion and metastasis of *MET*ex14.

Materials and Methods

Subjects

A total of 21,582 NSCLC formalin-fixed, paraffin-embedded tumor samples underwent an institutional review board-approved, retrospective analysis of tumor samples submitted for molecular profiling at a CLIA-certified genomics laboratory (Caris Life Sciences, Phoenix, AZ). Analyses included next-generation sequencing (NGS) of DNA (592 Gene Panel, NextSeq, or whole exome sequencing [WES], NovaSeq), RNA (NovaSeq, WTS), and immunohistochemistry (IHC) for PD-L1. Real-world survival information was obtained from insurance claims data and calculated from tissue collection or first of treatment time to last of contact. Kaplan-Meier estimates were calculated for molecularly defined patient cohorts.

DNA NGS, WES, and RNA WTS

DNA sequencing was performed using the NextSeq or NovaSeq platform (Illumina, Inc., San Diego, CA) after microdissection. Identified genetic variants were further annotated as "pathogenic," "likely pathogenic," "variant of unknown significance," "likely benign," or "benign," according to the 2015 American College of Medical Genetics and Genomics standards,[19] a core foundation for a recently published guideline for classifying oncogenicity of somatic variants.[20] Only "pathogenic" and "likely pathogenic" mutations were counted toward mutation frequency calculation in our study. A hybrid-capture method using Agilent SureSelect Human All Exon V7 bait panel (Agilent Technologies, Santa Clara, CA) and the Illumina NovaSeq platform (Illumina, Inc., San Diego, CA) were used for RNA sequencing. A minimum of 10% tumor content in the area for microdissection was required for enrichment and extraction of tumor-specific RNA. If no correlative DNA alteration was identified, *MET*ex14 required a read depth of at least 10. FASTQ files were aligned with STAR aligner (Alex Dobin, release 2.7.4a GitHub). Data were then produced by Salmon, which provides fast and bias-aware quantification of transcript expression.[21] BAM files from STAR aligner were processed for RNA variants using a proprietary custom detection pipeline. The reference genome was GRCh37/hg19.

Tumor Mutational Burden, PD-L1 Status

All nonsynonymous missense, nonsense, in-frame insertion/deletion and frameshift mutations that had not been previously described as germline alterations in dbSNP151, Genome Aggregation Database or benign variants were counted toward tumor mutational burden (TMB) measurement.[22] A cutoff point of more than or equal to 10 mutations per megabase (mut/Mb) was used to define TMB-high tumors. PD-L1 status was assessed by means of 22c3 anti–PD-L1 antibody (Dako) on formalin-fixed, paraffin-embedded sessions and evaluated for percentage positively stained tumor cells to derive a tumor proportion score.

Single-Sample Gene Enrichment Analysis

Single-sample gene enrichment analysis (ssGSEA) was used to calculate pathway enrichment scores of 50 hallmark gene pathways per tumor using WTS data set without normalization.[23,24] Interferon (IFN)-γ signature and T-cell inflammation signature scores were defined by 18-gene[25] and 160-gene mRNA signatures,[26] respectively, and were used to estimate the likelihood of a tumor's response to anti–programmed cell death protein-1 (PD-1) therapy. QuanTISeq was performed to quantify fractions of 10 different types of infiltrated immune cells.[27]

Statistical Methods

Chi-square and Fisher's exact tests were used to assess statistical differences between categorical variables and Wilcoxon or Mann-Whitney *U* tests for comparisons between numerical variables. Benjamin-Hochberg correction was applied to minimize the false discovery rate when multiple tests were performed, where the reported *p* or q value was the statistic without or with correction, respectively. R (version 4.1.2) was used for ssGSEA analysis and QuanTISeq. Python (version 3.9.12) was used for other analyses.

Results

Clinicopathologic Features

Of the 21,582 cases, 533 (2.47%) were identified with *MET*ex14 and 21,049 without *MET*ex14 (wild type [WT]) (Table 1). *MET*ex14-positive tumors occurred more frequently in females (302, 56.7% versus 231, 43.3% males, $p < 0.05$) and in older patients (median 77 y versus 69 y, $p < 0.0001$). The most frequently represented histology was adenocarcinoma (324, 60.8%), followed by squamous cell (57, 10.7%), adenosquamous (15, 2.8%), sarcomatoid (21, 3.9%), and large cell (1, 0.2%). Of all histologies, *MET*ex14 was enriched in patients with sarcomatoid histology (21 of 202, 10.4%) followed by adenosquamous (15 of 196, 7.65%). A total of 115 cases (21.6%) were classified as "other non-small cell carcinoma" histology in which accurate histologic information was not available or was of mixed histology. Staging information was unavailable; however, *MET*ex14 was more often identified through primary site of biopsy. Of the 104 patients with *MET*ex14 with smoking data, there was a higher proportion of light or never smokers compared with patients with WT ($p < 0.0001$).

Table 1. Clinicopathologic Characteristics of Patients With NSCLC With and Without *MET*ex14

Characteristic	Total N	*MET*ex14 skipping		P-value
	21582	Positive (n=533)	Negative (n=21049)	
Gender, n (%)				
Male	50.5% (10900/21582)	43.3% (231/533)	50.7% (10669/21049)	<0.05
Female	49.5% (10682/21582)	56.7% (302/533)	49.3% (10380/21049)	
Age at specimen collection, median(range)	69.0 (21 - 90) [21582]	77.0 (41 - 90) [533]	69.0 (21 - 90) [21049]	<0.0001
smoking status, n (%)				
Light smoker (<15 pack year)	65.6% (4072/6211)	79.8% (83/104)	65.3% (3989/6107)	<0.0001
Current heavy smoker	30.4% (1889/6211)	6.7% (7/104)	30.8% (1882/6107)	
Never smoker	4.0% (250/6211)	13.5% (14/104)	3.9% (236/6107)	
Histologies				
Adenocarcinoma	59.1% (12747/21582)	60.8% (324/533)	59.0% (12423/21049)	<0.001
Squamous	22.7% (4906/21582)	10.7% (57/533)	23.0% (4849/21049)	
Adenosquamous	0.9% (196/21582)	2.8% (15/533)	0.9% (181/21049)	
Sarcomatoid	0.9% (202/21582)	3.9% (21/533)	0.9% (181/21049)	
Large cell	0.3% (57/21582)	0.2% (1/533)	0.3% (56/21049)	
Others	16.1% (3474/21582)	21.6% (115/533)	16.0% (3359/21049)	
Site of biopsy				
Primary	55.5% (11968/21582)	64.5% (344/533)	55.2% (11624/21049)	<0.001
Metastatic	43.5% (9383/21582)	34.5% (184/533)	43.7% (9199/21049)	
Unknown	1.00% (216/21582)	1.00% (5/533)	1.1% (226/21049)	

Subtype of Genomic Alterations of METex14

To better understand the heterogeneity of *MET* mutations which yield *MET*ex14, we characterized the subtypes of *MET* mutations by their spatial chromosomal locations (Fig. 1*A*). The most common genomic alterations were base substitutions in the splice donor site (49.5%), located in 5′ splice site of intron 14, followed by deletions in the polypyrimidine tract (17.6%), located in intron 13, which play a role in spliceosome assembly, and deletions in the splice donor site (16.5%)

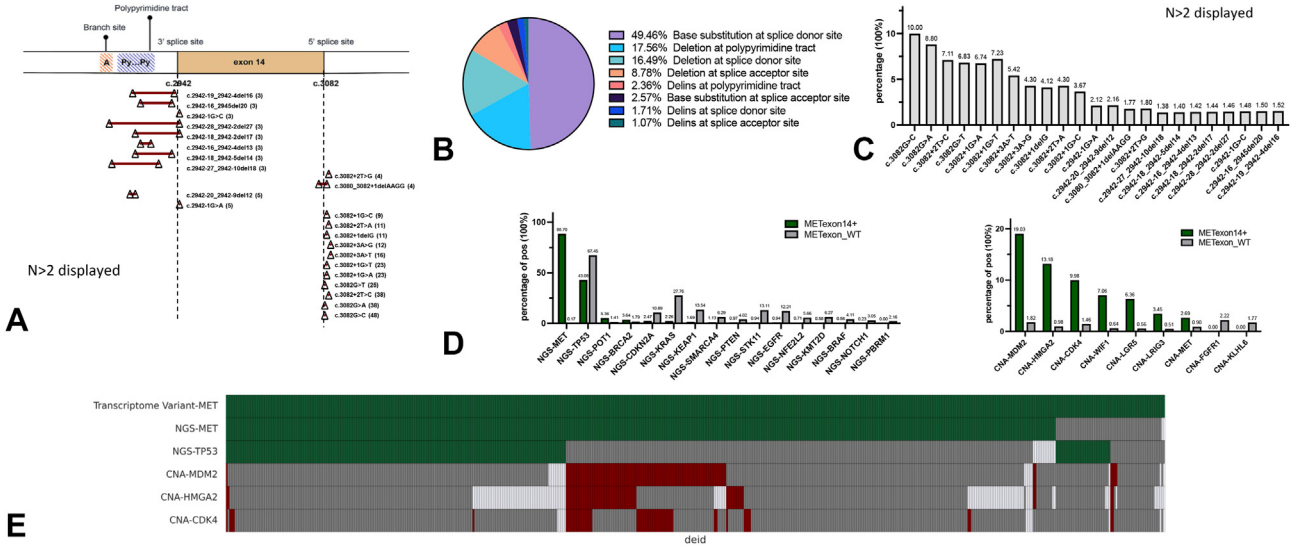

Figure 1. (*A*) Spatial chromosomal representation of *MET*ex14 mutation subtypes. (*B*) Distribution of *MET*ex14 alteration on the basis of mutation subtype. (*C*) Frequency of often identified DNA alterations. (*D*) Frequency of co-alterations (left) or co-amplifications (right) of *MET*ex14 and *MET* WT. (*E*) Oncoprint of *MET*ex14 and co-alterations in *TP53*, *MDM2*, *CDK4*, and *HMGA2* (green: mutation detected; red: amplification detected; gray: wild type; white: data not available). CNA $\geq$ 6. CNA, copy number alteration; *MET*ex14, *MET* exon 14; NGS, next-generation sequencing; WT, wild type.

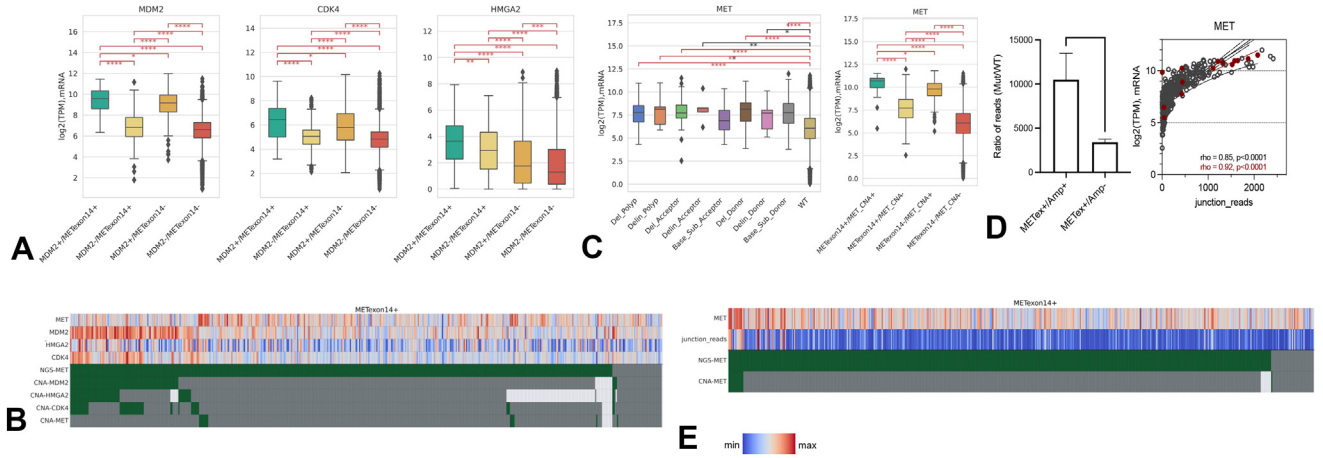

Figure 2. (*A*) mRNA expression of *MDM2*, *CDK4*, and *HMGA2* on the basis of *MDM2* co-amplification in *MET*ex14 and *MET* WT (y axis, log_2-transformed TPM; error bars represented interquartile range and median presented). (*B*) Oncoprint of *MDM2*, *CDK4*, and *HMGA2* represented with mRNA expression levels. Red indicates higher expression and blue lower expression. (*C*) *MET* expression on the basis of *MET*ex14 mutation subtype (left) and *MET* co-amplification (right). (*D*) Ratios of *MET*ex14 mutation junction reads to WT junction reads in *MET*ex14/Amp+ versus *MET*ex14/Amp- (left) and Spearman correlation (right) of *MET* expression and ratio of *MET*ex14 junction reads to WT junction reads (gray dots: *MET*ex14/Amp-; red dots: *MET*ex14/Amp+). (*E*) Oncoprint of *MET*ex14 and *MET* co-amplification represented against *MET* expression and *MET*ex14 junction reads. Amp, amplification; *MET*ex14, *MET* exon 14; TPM, Trusted Platform Module; WT, wild type.

(Fig. 1*B*). Less common alterations were deletions in splice acceptor site (8.8%), located in 3′ splice site of intron 13, insertions and deletions (indels) at poly-pyrimidine tract (2.4%), base substitutions at splice acceptor site (2.6%), indels at splice donor site (1.7%), and indels at splice acceptor site (1.1%). The most common alteration overall was c.3082G > C (Fig. 1*C*). Y1003X, a rare alteration directly affecting the Y1003 Cbl-binding sites, was found to be mutually exclusive to *MET*ex14 skipping variants ($p < 0.01$).

Of the 533 fusion variants identified by WTS, 11.3% did not have a corresponding genetic alteration, regardless of sequencing platform (Fig. 1*E* and Supplementary Fig. 1). Although speculative, this lack of corresponding fusion variant to its genomic alternation may be explained by possible alterations occurring within introns 13 and 14 that were distant from the skipped event, which would not be captured by the WES platform. In addition, oncogenic events with low allele frequency at the DNA level that may not be captured in the WES platform may also gain transcription advantage and overexpress above the detection level in WTS.

Co-alterations and Co-amplifications

*MET*ex14 skipping variants were largely mutually exclusive with other known driver mutations, including *KRAS*, *EGFR*, *BRAF*, *ALK* fusion, and *ROS-1* fusion (Fig. 1*D*). Co-alterations with *TP53* were represented in 43.1% of *MET*ex14 (67.5% WT) and 5.4% of *MET*ex14 were associated with *POT1* mutation (1.4% WT). Furthermore, 2.7% of patients with *MET*ex14 had *MET* co-amplifications (copy number alteration [CNA] ≥ 6), of which 0.19% also had *EGFR* alterations compared with 0.12% in *MET* WT, which may represent mechanisms of *EGFR* resistance. The most common co-alteration that distinguished *MET*ex14 from WT were co-amplifications (CNA ≥6) in three genes mapping to chromosome 12q14–15–*MDM2* (12q15) (19.0% versus 1.8% WT), *HMGA2* (12q14.3) (13.2% versus 0.98% WT), and *CDK4* (12q14.1) (10.0% versus 1.5% WT) (Fig. 1*D*). Frequent co-amplification of *MDM2* in *MET*ex14 compared with *MET* WT suggests *MDM2* as an important event in *MET* skipping variants. As expected, *MDM2* amplification was mutually exclusive to *TP53* alterations (Fig. 1*E*). No considerable differences in co-alterations between WES and 592 gene panel platforms were observed in our cohort (Supplementary Fig. 1).

The functional relevance of co-amplification of *MDM2*, *CDK4*, and *HMGA2* were further assessed by correlation with RNA expression. As anticipated, *MDM2* amplification correlated with higher *MDM2* expression levels than in nonamplified cases and also higher *CDK4* and *HMGA2* expression (Fig. 2*A*). Amplification of *CDK4* was also associated with higher *CDK4*, *MDM2*, and *HMGA2* expression and *HMGA2* amplification correlated with increased expression of *HMGA2*, *MDM2*, and *CDK4* (Supplementary Fig. 2). In contrast to *MDM2* and *CDK4* in which amplification revealed positive correlation with expression, *HMGA2* amplification was not associated with expression (Fig. 2*B*). The correlation between gene amplification and expression in *MDM2* and *CDK4* and lack of correlation in *HMGA2* may point toward *MDM2* and *CDK4* as common and functionally relevant co-oncogenic events in *MET*ex14 tumors. *CDK4* co-

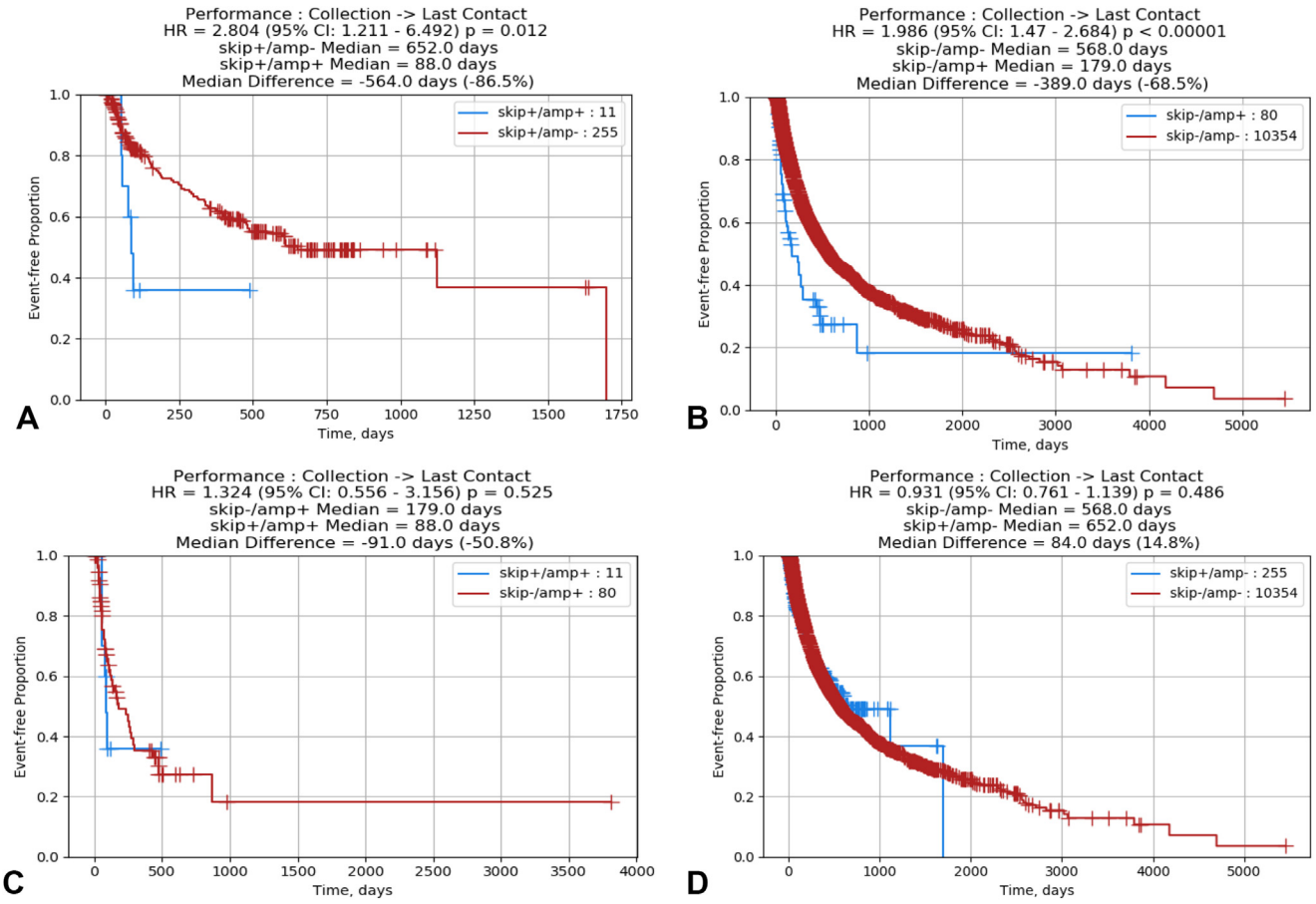

Figure 3. (*A*) Kaplan-Meier plot of overall survival (date of tissue collection to last contact) of *MET*ex14 patients with and without amplification. (*B*) Kaplan-Meier plot of overall survival (date of tissue collection to last contact) of *MET* WT patients with and without amplification. (*C*) Kaplan-Meier plot of overall survival (date of tissue collection to last contact) of *MET*-amplified patients with and without *MET*ex14. (*D*) Kaplan-Meier plot of overall survival (date of tissue collection to last contact) of non-*MET*-amplified patients with and without *MET*ex14. HR, hazard ratio; CI, confidence interval; *MET*ex14, *MET* exon 14; WT, wild type.

amplification resulted in relatively high *MDM2* expression regardless of *MDM2* co-amplification in *MET*ex14, which may suggest *CDK4* to be involved in regulation of *MDM2* expression (Supplementary Fig. 3).

MET mRNA Expression on the Basis of Alteration Type

A 3-fold increase in *MET* RNA expression in *MET*ex14 was observed compared with *MET* WT, with most splice site alteration subtypes (donor splice site base substitutions, donor splice site deletion, polypyrimidine site deletion, and acceptor splice site deletion) translating to significantly increased *MET* expression in (all $q < 0.01$) (Fig. 2*C*, left). A trend toward increased mRNA expression was observed in indels at splice donor site, polypyrimidine tract, and splice acceptor site ($p < 0.01$). There was no difference in *MET* expression between splice acceptor site base substitution and WT, which may suggest differential expression of *MET* on the basis of mutation subtype. Strikingly, co-amplification of *MET* with *MET*ex14 was observed to have a 24-fold increase in *MET* expression compared with double WT (*MET*ex14 WT and *MET* nonamplified tumor), with 13-fold increase in expression with *MET* amplification alone and a threefold increase in expression with *MET*ex14 (Fig. 2*C*, right). Within the *MET* co-amplified tumors, the *MET*ex14 allelic variant was preferentially expressed ($p < 0.01$, Fig. 2*D* and *E*), on the basis of increased number of *MET*ex14 junction reads compared with WT junction reads. In patients with available prognostic data, *MET* amplification was observed to be associated with worse overall survival compared with *MET*ex14 (Fig. 3).

Prognosis of Patients Treated With Crizotinib Based on Mutation Subtype

Among 25 patients whose treatment data with crizotinib were available, patients with donor splice site alterations were observed to have improved prognosis

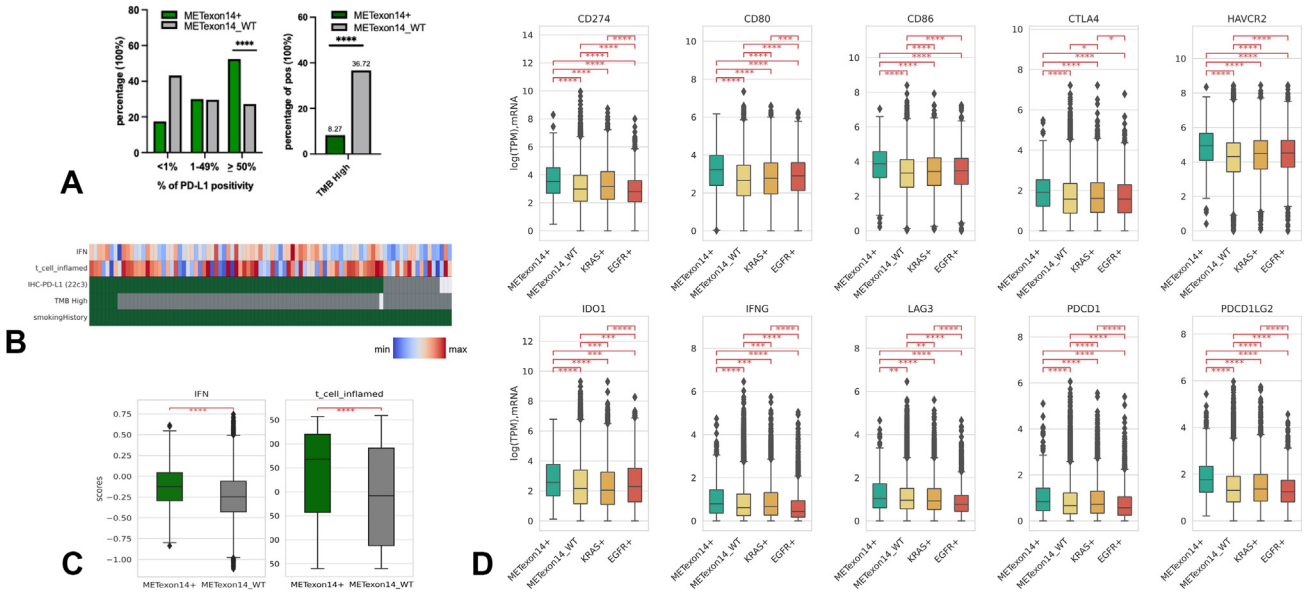

Figure 4. (*A*) *MET*ex14 and *MET* WT patients stratified by PD-L1 less than 1%, 1% to 49%, and greater than or equal to 50% (left). Percentage of patients with high TMB (≥10 mut/Mb) in *MET*ex14 and *MET* WT cohorts (right). (*B*) Oncoprint of *MET*ex14 with smoking history against TMB, PD-L1, IFN-γ signature, and T-cell inflammation signature. (*C*) IFN-γ signature (left) and T-cell inflammation signature (right) in *MET*ex14 and *MET* WT. (*D*) mRNA expression of immune checkpoints in *MET*ex14, *MET* WT, *KRAS* mutant, and *EGFR* mutant cohorts. IFN-γ, interferon-γ; *MET*ex14, *MET* exon 14; mut/Mb, mutations per megabase; PD-L1, programmed death-ligand 1; WT, wild type.

compared with patients with acceptor site alterations using start of treatment to last of contact (hazard ratio = 0.24, $p = 0.006$), suggesting possible differential response to treatment on the basis of mutation subtype (Supplementary Fig. 4). Co-alterations in copy number alteration of *WIF1*, *CDKN2A*, and *RB1* were more frequent in acceptor site alterations treated with crizotinib and no difference in immunogenic signatures was observed, though evaluation is limited by a small sample size (Supplementary Fig. 5). No difference in prognosis was observed between all patients, either treated or untreated, with donor splice site and acceptor splice site mutations, which may suggest mutation subtype as a potential predictive, but not a prognostic biomarker.

PD-L1 and TMB

Of 20,694 patients with available PD-L1 IHC data, nearly twice as many patients in the *MET*ex14 cohort had a high PD-L1 more than or equal to 50% (52.5% versus 27.3% WT, $q < 0.0001$) with similar proportions observed in the PD-L1 1% to 49% (30.0% versus 29.7% WT) (Fig. 4*A*, left). Of 21,152 patients with TMB status, lower proportion of *MET*ex14 patients had a high TMB (≥10 mut/Mb), (8.3% versus 36.7% WT) with median TMB, 4 mut/Mb *MET*ex14 and 7 mut/Mb WT ($q < 0.0001$) (Fig. 4*A*, right). A similar pattern of lower proportion of patients having median TMB greater than or equal to 15 mut/Mb and greater than or equal to 20 mut/Mb were observed in *MET*ex14 compared with WT (Supplementary Fig. 6). In addition, of seven *MET*ex14 patients with high TMB who had smoking status available, none were non-smokers (Fig. 4*B*) and of 2402 WT patients with high TMB, only 13 (0.5%) were non-smokers, highlighting high TMB correlating with smoking status. Every *MET*ex14 tumor with high TMB fell into the high PD-L1 greater than or equal to 50% strata.

Immune Infiltrate Signature

A previous proof-of-principle study revealed that an 18-gene mRNA signature associated with IFN-γ and T-cell inflammation predicted response to immunotherapy across multiple tumor types, and larger immunogenic gene signatures (160-gene) have also been established.[25,26] Variable outcomes with immunotherapy in *MET*ex14 as reported in the literature despite association with high PD-L1 prompted evaluation of tumor microenvironment (TME) in *MET*ex14 and WT subsets using the IFN-γ (18-gene) and T-cell inflammation signatures (160-gene) at the transcriptomic level. We found significant enrichment of IFN-γ and T-cell inflammation signatures in *MET*ex14 compared with WT (Fig. 4*C*). There was no significant difference in IFN-γ or T-cell inflammation signatures on the basis of smoking or high TMB (≥10 mut/Mb) status within *MET*ex14 which suggests smoking or TMB to not be confounding factors in explaining differences in inflammatory signatures (Supplementary Fig. 7*A* and *B*). Significantly higher IFN-

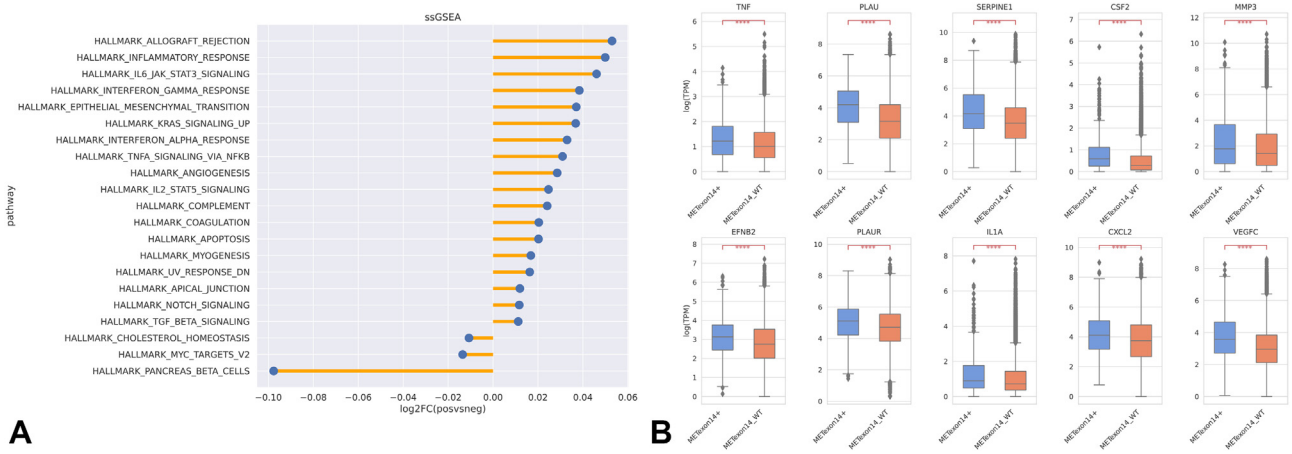

Figure 5. (*A*) ssGSEA pathway analysis of *MET*ex14 patients. (*B*) mRNA expression of genes previously found to be up-regulated in *MET*ex14 in in vitro models in *MET*ex14 and *MET* WT cohorts. *MET*ex14, *MET* exon 14; mut/Mb, mutations per megabase; FC, fold change; ssGSEA, single-sample gene enrichment analysis; WT, wild type.

γ signatures were observed with increasing PD-L1 expression in *MET*ex14 and *MET* WT (Supplementary Fig. 7*C*), with the difference in IFN-signatures more significant in the PD-L1 greater than or equal to 50% subgroups (Supplementary Fig. 7*D*). Moreover, *MET*ex14 also displayed significantly higher immune cell infiltrates of macrophage M1, macrophage M2, CD4+ T-cells, CD8+ T-cells, regulatory T-cells, and dendritic cells compared with WT (Supplementary Fig. 8).

Higher expression of IFN-γ previously revealed inhibition of immune activation through a negative feedback loop,[28] and multiple genes involved in immune checkpoints in addition to *CD274* (PD-L1), including *CD80*, *CD86*, *CTLA4*, *HAVCR2 (TIM-3)*, *LAG3*, *IDO1*, *PDCD1*, and *PDCD1LG2* were also more up-regulated in *MET*ex14 compared with WT (Fig. 4*D*). This increase in immune checkpoints was observed when compared against *KRAS* and *EGFR*-mutant cohorts suggesting a more immunosuppressive TME with *MET*ex14 compared with alternate driver mutations. A similar trend of higher PD-L1, lower TMB, higher IFN-γ/T-cell inflammation signatures, and higher immunosuppressive checkpoints was also observed in *MET*ex14 when compared with a cohort of pan-WT patients, who did not harbor co-alterations in *EGFR*, *KRAS*, *ALK*, and *ROS-1*, which could potentially affect immune TME (Supplementary Figs. 6 and 9). Strong association of higher IFN-γ and T-cell inflammation signatures in *MET*ex14 irrespective of smoking status or TMB and increased expression of multiple immune checkpoints suggest both an inflammatory and an immunosuppressive TME in *MET*ex14.

ssGSEA Pathway Analysis

To further explore differentially regulated pathways in *MET*ex14, we performed ssGSEA analysis and observed a consistent up-regulation of pathways involved in inflammatory response. In addition to up-regulation of IFN-γ, pathways involved in EMT, angiogenesis, and apical junction pathways were found to be enriched in *MET*ex14 on univariate analysis (Fig. 5*A*). When stratified by histology, EMT signature had a trend toward higher association with non-adenocarcinoma histologies (squamous, adenosquamous, and sarcomatoid) (Supplementary Fig. 10). mRNA expression of individual markers involved in invasion and metastases of *MET*, including *PLAU*, *SERPINE1*, *CSF2*, *MMP3*, *EFNB2*, *PLAUR*, *IL1A*, *CXCL2*, and *VEGFC*, which were up-regulated in our previously established preclinical cell-based models of *MET*ex14[18] was also found to be significantly overexpressed in *MET*ex14 patients ($q < 0.00001$ for all) (Fig. 5*B*). An up-regulation in tumor necrosis factor in *MET*ex14 was observed, which was not observed in our previous preclinical model.[18] On 70 cases with data available for logistic regression on multivariate analysis, apical junction pathway was observed to be associated with *MET*ex14 ($p < 0.05$). These up-regulated pathways and genes highlight several potential vulnerabilities that can be explored for potential therapeutic benefit.

Discussion

We present the most comprehensive characterization of *MET*ex14 alterations to date encompassing 533 *MET*ex14 tumors using WTS data. Similar to previous cohorts identified through DNA genomic profiling, patients with *MET*ex14 skipping were predominantly female, older, and enriched in sarcomatoid and adenosquamous histologies.[3,4,9,13,29,30] This is in contrast to other driver alterations such as *EGFR* and *ALK*, which are associated with younger age and adenocarcinoma,

and suggests the importance of unbiased NGS testing in patients irrespective of age or adenocarcinoma histology.[31] Association of smoking status with *MET*ex14 has previously widely varied,[3,4,9,13,29,32] and in our limited cohort of patients whose smoking status was available, *MET*ex14 patients were predominantly of light smokers (<15 pack years) or nonsmokers, though data were lacking on previous heavy (≥15 pack years) smokers.

The frequency and subtype of genomic alterations of *MET*ex14 were also comparable to previous DNA profiling data, with *MET*ex14 identified in 2.47% by WTS and the donor splice site base substitutions as the most common alteration leading to a skipped variant.[2,3,9,11,17,32] Approximately 11% of patients with a skipped variant had no associated DNA alteration, which may be secondary to underlying long deletions not captured owing to limitations in detection, and support RNA-based testing as a more sensitive assay for *MET*ex14.[15,16] Near mutual exclusivity was observed with *KRAS* and *EGFR* mutations supporting *MET*ex14 as an independent oncogenic driver,[2,9] and co-mutations were common in *TP53* and *POT1*. *POT1* (protection of telomeres 1), responsible for telomere maintenance, is enriched in pulmonary sarcomatoid subtypes, and its co-alteration with *MET*ex14 may represent histologic association.[33]

A novel observation of differential *MET* expression on the basis of mutation subtype was reported in our study, with at least three-fold increase in expression in nearly all mutation subtypes, except for point mutations in splice acceptor site. Although crizotinib,[11] capmatinib,[10] and tepotinib[12] have not revealed disparate treatment response on the basis of mutation subtypes, molecular characterization among splicing mutations in these studies was more broadly categorized and not uniformly defined across studies. Thus, whether observed differences in mRNA expression on the basis of splicing mutation subtypes may have treatment implications requires further understanding. A more striking finding in our study was that in cases with *MET* co-amplification (CNA ≥ 6), a near 24-fold increase in *MET* expression was found, higher than 14-fold increase with *MET* amplification alone and three-fold increase with *MET*ex14 alone, suggesting synergistic *MET* expression with *MET* co-amplification. The clinical significance of this increased *MET* expression with *MET* co-amplification may be both prognostic and therapeutic. *MET* amplification was previously associated with strong c-MET expression and poor prognosis, also revealed in our study on the basis of worse survival curves in patients with *MET* amplification.[9] Both capmatinib[10] and crizotinib[34] were found to have an increased response rate with high levels of *MET* amplification and support high-level *MET* amplification as a possible prognostic and predictive biomarker. Interestingly, co-amplification of *MET* with *MET*ex14 did not have an increased response to capmatinib,[10] but it did have high response rates of more than 60% to tepotinib.[12] Nevertheless, levels of co-amplification were not reported in these studies. Whether high-level co-amplification, which correlates with higher mRNA expression and presumably higher protein expression, that in a previous study revealed improved response to MET tyrosine kinase inhibitor (TKI),[35] can serve as a predictive biomarker, warrants further investigation.

Dysregulation of p53 has well been associated in lung cancer.[36] Inactivation of p53 can occur in multiple ways, including mutation of *TP53* or inactivation of WT p53, such as through *MDM2* amplification, a negative regulator of p53. Our study revealed a significantly higher *MDM2* amplification in *MET*ex14 which was also observed in previous DNA profiling studies.[2,4,13,17] As anticipated, *MDM2* co-amplification was mutually exclusive to *TP53* mutation and despite lower *TP53* mutations found in *MET*ex14 compared with *MET* WT, the high combined proportion of patients having either mutant *TP53* (43.08%) or *MDM2* amplification (19.03%) in *MET*ex14 highlights impaired TP53 pathway as a crucial actionable target and driver of oncogenesis in *MET*ex14. Co-amplifications in *HMGA2* was not previously reported and its frequent co-amplification with *MET*ex14 highlights the role of *HMGA2*, which promotes EMT through transforming growth factor-β/Smads, PI3K/AKT, and Wnt/B-catenin pathways,[37] as a functionally relevant gene important in the invasive properties of *MET*ex14.

Interestingly, the most frequent co-amplified genes, *MDM2*, *CDK4*, and *HMGA2*, all co-localized to chromosome 12q14–15. *MDM2* and *CDK4* seemed co-dependent of each other, on the basis of increased expression of *CDK4* with *MDM2* amplification and increased expression of *MDM2* with *CDK4* amplification. *CDK4* amplification resulted in high *MDM2* expression regardless of *MDM2* amplification in *MET*ex14, and this finding could suggest *CDK4* as an important regulator of *MDM2*. Both MDM2 inhibitors and CDK4/6 inhibitors have antitumor activity in alternate tumor types when combined with chemotherapy,[38] targeted therapy,[39,40] and hormonal therapy,[41] and reveal potential novel combination treatment strategies with MET TKI in *MET*ex14 patients with *MDM2* or *CDK4* co-amplification.

Despite high PD-L1 expression, patients with *MET*ex14 were found to have in published series low to modest responses to immunotherapy.[13,14,42,43] Low TMB in *MET*ex14 compared with WT was observed in our cohort, in which only 8% of *MET*ex14 had high TMB (≥10 mut/Mb) and may possibly explain lower than expected responses to immunotherapy in *MET*ex14

despite high PD-L1 expression. Furthermore, higher expression of immunosuppressive checkpoints was observed in *MET*ex14 compared with WT, contributing to potential bypass pathways conferring resistance to anti–PD-1/PD-L1. Interestingly, *MET*ex14 was also observed to have higher IFN-γ/T-cell inflammatory gene signatures compared with WT, and both an up-regulation of inflammatory and immunosuppressive TME in patients previously known to only have modest responses to immunotherapy could suggest immune suppression as a dominating mechanism in *MET*ex14. On the basis of promising data of combination checkpoint inhibitors in NSCLC,[44] combination immunotherapy with MET TKI may be potential therapeutic strategies in overcoming anti–PD-L1/PD-1 resistance.

Last, consistent with our previous preclinical studies,[18] an up-regulation of genes related to cellular adhesion, extracellular matrix disassembly, and angiogenesis, mechanisms of invasion and metastases in *MET*ex14 were also up-regulated in our *MET*ex14 cohort by pathway analysis. Tumor angiogenesis is hypothesized to promote an immunosuppressive environment[45] and may serve as an additional factor in immunotherapy resistance in *MET*ex14. Efficacy of dual driver-alteration and vascular endothelial growth factor (VEGF)-inhibition in NSCLC have been found with first-line EGFR inhibitor, erlotinib,[46,47] and in preclinical studies with c-MET and VEGF/vascular epithelial growth factor receptor (VEGFR) in epithelial cancers.[48] Combination anti-VEGF therapy and MET-directed TKI with or without immunotherapy may thus be potential alternate treatment strategies in improving treatment outcomes in *MET*ex14 which rely on angiogenesis for invasion and metastases.

Limitations of our study include the inclusion of alternate driver mutations in *MET*ex14 and *MET* WT, which may confound results; however, most cohort designated as WT did not have an alternate driver mutation and the focus of the study was to characterize *MET*ex14 against samples without *MET*ex14. In addition, although *MET* mRNA expression was differentially up-regulated with distinct *MET*ex14 mutation subtypes and synergistically increased with *MET* co-amplification, whether this translates into increased c-MET expression and improved response to novel MET TKI remains to be further characterized with IHC and detailed treatment data. The variability of time in tissue collection, pre-treatment versus post-treatment, also may confound characterization of co-alterations or results on immune TME because co-alterations may represent bypass resistance mechanisms rather than *de novo* co-mutations and up-regulation of checkpoint inhibition may be a response to immunotherapy, respectively, in those treated with immunotherapy. Overall, an improved understanding of *MET*ex14 subsets is needed to select patients who may have improved responses to MET TKI, and for those patients with suboptimal response, further research on newer combination treatment strategies such as MET TKI with anti-VEGF, selective small molecule inhibitors of MDM-2 and CDK4/6, or with combination checkpoint inhibitors are needed.

CRediT Authorship Contribution Statement

So Yeon Kim: Conceptualization, Methodology, Analysis, Investigation, Original draft preparation, Writing—review and editing.

Jun Yin: Data curation, Methodology, Analysis, Software, Investigation, Visualization, Writing—review and editing.

Stephen Bohlman: Analysis.

Phillip Walker, Sanja Dacic, Chul Kim, Hina Khan, Stephen V. Liu, Patrick C. Ma, Misako Nagasaka, Karen L. Reckamp, Jim Abraham, Dipesh Uprety, Joanne Xiu: Writing—review and editing.

Feng Wang: Conceptualization.

Jian Zhang: Data curation, Investigation.

Haying Cheng: Writing—review and editing, Supervision.

Balazs Halmos: Conceptualization, Methodology, Analysis, Investigation, Writing—review and editing, Supervision.

Supplementary Data

Note: To access the supplementary material accompanying this article, visit the online version of the *JTO Clinical and Research Reports* at www.jtocrr.org and at https://doi.org/10.1016/j.jtocrr.2022.100381.

References

1. Ma PC, Jagadeeswaran R, Jagadeesh S, et al. Functional expression and mutations of c-Met and its therapeutic inhibition with SU11274 and small interfering RNA in non-small cell lung cancer. *Cancer Res*. 2005;65:1479–1488.
2. Frampton GM, Ali SM, Rosenzweig M, et al. Activation of MET via diverse exon 14 splicing alterations occurs in multiple tumor types and confers clinical sensitivity to MET inhibitors. *Cancer Discov*. 2015;5:850–859.
3. Schrock AB, Frampton GM, Suh J, et al. Characterization of 298 patients with lung cancer harboring MET exon 14 skipping alterations. *J Thorac Oncol*. 2016;11:1493–1502.
4. Awad MM, Oxnard GR, Jackman DM, et al. MET exon 14 mutations in non-small-cell lung cancer are associated with advanced age and stage-dependent MET genomic amplification and c-met overexpression. *J Clin Oncol*. 2016;34:721–730.
5. Zhang Y, Xia M, Jin K, et al. Function of the c-Met receptor tyrosine kinase in carcinogenesis and associated therapeutic opportunities. *Mol Cancer*. 2018;17:45.

6. Kong-Beltran M, Seshagiri S, Zha J, et al. Somatic mutations lead to an oncogenic deletion of met in lung cancer. *Cancer Res*. 2006;66:283–289.
7. Vuong HG, Ho ATN, Altibi AMA, Nakazawa T, Katoh R, Kondo T. Clinicopathological implications of MET exon 14 mutations in non-small cell lung cancer—a systematic review and meta-analysis. *Lung Cancer*. 2018;123:76–82.
8. Yeung SF, Tong JHM, Law PPW, et al. Profiling of oncogenic driver events in lung adenocarcinoma revealed MET mutation as independent prognostic factor. *J Thorac Oncol*. 2015;10:1292–1300.
9. Tong JH, Yeung SF, Chan AW, et al. MET amplification and exon 14 splice site mutation define unique molecular subgroups of non-small cell lung carcinoma with poor prognosis. *Clin Cancer Res*. 2016;22:3048–3056.
10. Wolf J, Seto T, Han JY, et al. Capmatinib in MET exon 14–mutated or MET-amplified non–small-cell lung cancer. *N Engl J Med*. 2020;383:944–957.
11. Drilon A, Clark JW, Weiss J, et al. Antitumor activity of crizotinib in lung cancers harboring a MET exon 14 alteration. *Nat Med*. 2020;26:47–51.
12. Paik PK, Felip E, Veillon R, et al. Tepotinib in non–small-cell lung cancer with MET exon 14 skipping mutations. *N Engl J Med*. 2020;383:931–943.
13. Lee JK, Madison R, Classon A, et al. Characterization of non–small-cell lung cancers with MET exon 14 skipping alterations detected in tissue or liquid: clinicogenomics and real-world treatment patterns. *JCO Precis Oncol*. 2021;5:PO.21.00122.
14. Sabari JK, Leonardi GC, Shu CA, et al. PD-L1 expression, tumor mutational burden, and response to immunotherapy in patients with MET exon 14 altered lung cancers. *Ann Oncol*. 2018;29:2085–2091.
15. Davies KD, Lomboy A, Lawrence CA, et al. DNA-based versus RNA-based detection of MET exon 14 skipping events in lung cancer. *J Thorac Oncol*. 2019;14:737–741.
16. Benayed R, Offin M, Mullaney K, et al. High yield of RNA sequencing for targetable kinase fusions in lung adenocarcinomas with no mitogenic driver alteration detected by DNA sequencing and low tumor mutation burden. *Clin Cancer Res*. 2019;25:4712–4722.
17. Awad MM, Lee JK, Madison R, et al. Characterization of 1,387 NSCLCs with MET exon 14 (METex14) skipping alterations (SA) and potential acquired resistance (AR) mechanisms. *J Clin Oncol*. 2020;38(suppl 15): 9511–9511.
18. Wang F, Liu Y, Qiu W, et al. Functional analysis of MET exon 14 skipping alteration in cancer invasion and metastatic dissemination. *Cancer Res*. 2022;82:1365–1379.
19. Richards S, Aziz N, Bale S, et al. Standards and guidelines for the interpretation of sequence variants: a joint consensus recommendation of the American College of Medical Genetics and Genomics and the Association for Molecular Pathology. *Genet Med*. 2015;17:405–424.
20. Horak P, Griffith M, Danos AM, et al. Standards for the classification of pathogenicity of somatic variants in cancer (oncogenicity): joint recommendations of Clinical Genome Resource (ClinGen), Cancer Genomics Consortium (CGC), and Variant Interpretation for Cancer Consortium (VICC). *Genet Med*. 2022;24:986–998.
21. Patro R, Duggal G, Love MI, Irizarry RA, Kingsford C. Salmon provides fast and bias-aware quantification of transcript expression. *Nat Methods*. 2017;14:417–419.
22. Merino DM, McShane LM, Fabrizio D, et al. Establishing guidelines to harmonize tumor mutational burden (TMB): in silico assessment of variation in TMB quantification across diagnostic platforms: phase I of the Friends of Cancer Research TMB Harmonization Project. *J Immunother Cancer*. 2020;8:e000147.
23. Subramanian A, Tamayo P, Mootha VK, et al. Gene set enrichment analysis: a knowledge-based approach for interpreting genome-wide expression profiles. *Proc Natl Acad Sci U S A*. 2005;102:15545–15550.
24. Mootha VK, Lindgren CM, Eriksson KF, et al. PGC-1 α-responsive genes involved in oxidative phosphorylation are coordinately downregulated in human diabetes. *Nat Genet*. 2003;34:267–273.
25. Ayers M, Lunceford J, Nebozhyn M, et al. IFN-γ-related Mrna profile predicts clinical response to PD-1 blockade. *J Clin Invest*. 2017;127:2930–2940.
26. Spranger S, Luke JJ, Bao R, et al. Density of immunogenic antigens does not explain the presence or absence of the T-cell-inflamed tumor microenvironment in melanoma. *Proc Natl Acad Sci U S A*. 2016;113:E7759–E7768.
27. Finotello F, Mayer C, Plattner C, et al. Molecular and pharmacological modulators of the tumor immune contexture revealed by deconvolution of RNA-seq data. *Genome Med*. 2019;11:34.
28. Bellucci R, Martin A, Bommarito D, et al. Interferon-γ-induced activation of JAK1 and JAK2 suppresses tumor cell susceptibility to NK cells through upregulation of PD-L1 expression. *Oncoimmunology*. 2015;4:e1008824.
29. Kim EK, Kim KA, Lee CY, et al. Molecular diagnostic assays and clinicopathologic implications of MET exon 14 skipping mutation in non-small-cell lung cancer. *Clin Lung Cancer*. 2019;20:e123–e132.
30. Rahouma M, Kamel M, Narula N, et al. Pulmonary sarcomatoid carcinoma: an analysis of a rare cancer from the Surveillance, Epidemiology, and End Results database. *Eur J Cardiothorac Surg*. 2017;53:828–834.
31. Sacher AG, Dahlberg SE, Heng J, Mach S, Jänne PA, Oxnard GR. Association between younger age and targetable genomic alterations and prognosis in non-small-cell lung cancer. *JAMA Oncol*. 2016;2:313–320.
32. Le X, Hong L, Hensel C, et al. Landscape and clonal dominance of co-occurring genomic alterations in non-small-cell lung cancer harboring MET exon 14 skipping. *JCO Precis Oncol*. 2021;5:PO.21.00135.
33. Shen E, Xiu J, Bentley R, López GY, Walsh KM. Frequent mutations of POT1 distinguish pulmonary sarcomatoid carcinoma from other lung cancer histologies. *Clin Lung Cancer*. 2020;21:e523–e527.
34. Camidge DR, Otterson GA, Clark JW, et al. Crizotinib in patients with MET amplified NSCLC. *J Thorac Oncol*. 2021;16:1017–1029.
35. Guo R, Offin M, Brannon AR, et al. MET Exon 14-altered lung cancers and MET inhibitor resistance. *Clin Cancer Res*. 2021;27:799–806.
36. Momand J, Jung D, Wilczynski S, Niland J. The MDM2 gene amplification database. *Nucleic Acids Res*. 1998;26:3453–3459.

37. Zhang S, Mo Q, Wang X. Oncological role of HMGA2 (review). *Int J Oncol*. 2019;55:775–788.
38. Konopleva MY, Röllig C, Cavenagh J, et al. Idasanutlin plus cytarabine in relapsed or refractory acute myeloid leukemia: results of the MIRROS trial. *Blood Adv*. 2022;6:4147–4156.
39. Liu M, Xu S, Wang Y, et al. PD 0332991, a selective cyclin D kinase 4/6 inhibitor, sensitizes lung cancer cells to treatment with epidermal growth factor receptor tyrosine kinase inhibitors. *Oncotarget*. 2016;7:84951–84964.
40. Wang Y, Li X, Liu X, et al. Simultaneous inhibition of PI3Kα and CDK4/6 synergistically suppresses KRAS-mutated non-small cell lung cancer. *Cancer Biol Med*. 2019;16:66–83.
41. Hortobagyi GN, Stemmer SM, Burris HA, et al. Overall survival with ribociclib plus letrozole in advanced breast cancer. *N Engl J Med*. 2022;386:942–950.
42. Mazieres J, Drilon A, Lusque A, et al. Immune checkpoint inhibitors for patients with advanced lung cancer and oncogenic driver alterations: results from the IMMUNOTARGET registry. *Ann Oncol*. 2019;30:1321–1328.
43. Guisier F, Dubos-Arvis C, Viñas F, et al. Efficacy and safety of anti-PD-1 immunotherapy in patients with advanced NSCLC with BRAF, HER2, or MET mutations or RET translocation: GFPC 01-2018. *J Thorac Oncol*. 2020;15:628–636.
44. Paz-Ares L, Ciuleanu TE, Cobo M, et al. First-line nivolumab plus ipilimumab combined with two cycles of chemotherapy in patients with non-small-cell lung cancer (CheckMate 9LA): an international, randomized, open-label, phase 3 trial. *Lancet Oncol*. 2021;22:198–211.
45. Huang Y, Goel S, Duda DG, Fukumura D, Jain RK. Vascular normalization as an emerging strategy to enhance cancer immunotherapy. *Cancer Res*. 2013;73:2943–2948.
46. Nakagawa K, Garon EB, Seto T, et al. Ramucirumab plus erlotinib in patients with untreated, EGFR-mutated, advanced non-small-cell lung cancer (RELAY): a randomized, double-blind, placebo-controlled, phase 3 trial. *Lancet Oncol*. 2019;20:1655–1669.
47. Kawashima Y, Fukuhara T, Saito H, et al. Bevacizumab plus erlotinib versus erlotinib alone in Japanese patients with advanced, metastatic, EGFR-mutant non-small-cell lung cancer (NEJ026): overall survival analysis of an open-label, randomized, multicentre, phase 3 trial. *Lancet Respir Med*. 2022;10:72–82.
48. Awazu Y, Nakamura K, Mizutani A, et al. A novel inhibitor of c-Met and VEGF receptor tyrosine kinases with a broad spectrum of in vivo antitumor activities. *Mol Cancer Ther*. 2013;12:913–924.